

Experimental studies and nuclear model calculations on (p, xn) and (p, pxn) reactions on ^{85}Rb from their thresholds up to 100 MeV

By S. Kastleiner¹, Yu. N. Shubin^{1,a}, F. M. Nortier^{2,b}, T. N. van der Walt² and S. M. Qaim^{1,*}

¹ Institut für Nuklearchemie, Forschungszentrum Jülich GmbH, D-52425 Jülich, Germany

² Radionuclide Production Group, iThemba LABS, Somerset West 7129, South Africa

(Received December 12, 2003; accepted in revised form March 4, 2004)

*Proton induced reaction / Excitation function /
Experimental study via stacked-foil technique /
Nuclear model calculation / Isomeric cross section ratio*

Summary. Excitation functions were measured by the stacked-foil technique for the reactions $^{85}\text{Rb}(p, pxn)^{84\text{m},\text{g},83,82\text{m},81}\text{Rb}$ from their thresholds up to 100 MeV. Nuclear model calculations were performed using the code ALICE-IPPE both on (p, xn) reactions reported earlier and (p, pxn) reactions described here. The experimental excitation curves and the results of nuclear model calculations were found to be qualitatively in agreement. With the exception of the (p, n) reaction above 40 MeV, the theory appears to reproduce all the experimental data within deviations of about 50%. The cross section ratios for the isomeric pairs $^{85\text{m},\text{g}}\text{Sr}$ and $^{84\text{m},\text{g}}\text{Rb}$ are discussed qualitatively in terms of the spins of the states involved and the increasing projectile energy.

1. Introduction

A knowledge of excitation functions of charged particle induced reactions is of considerable significance for defining optimum conditions for production of some medically important radionuclides at accelerators as well as for testing nuclear models. Of particular interest is the intermediate energy range of 30 to 100 MeV where, for many target nuclei, the experimental data base is still rather weak.

The excitation functions of proton induced reactions on ^{85}Rb were investigated previously in connection with the production of ^{81}Sr [1] and ^{82}Sr [2]. We recently published [3] the excitation functions of $^{85}\text{Rb}(p, xn)^{85\text{m},\text{g},83,82,81}\text{Sr}$ reactions up to 100 MeV and discussed the results in terms of yields and purities of two medically important radionuclides ^{82}Sr and ^{83}Sr , when produced *via* the $^{85}\text{Rb}(p, 4n)^{82}\text{Sr}$ and $^{85}\text{Rb}(p, 3n)^{83}\text{Sr}$ reactions, respectively. Now we report on the excitation functions of the $^{85}\text{Rb}(p, pxn)^{84\text{m},\text{g},83,82\text{m},81}\text{Rb}$ reactions obtained in the same experiments. The product nuclei and the decay data used [cf. 4] are given in Table 1.

* Author for correspondence (E-mail: s.m.qaim@fz-juelich.de).

^a Guest scientist from Institute of Physics and Power Engineering (IPPE), Obninsk, Russia.

^b Present address: Los Alamos National Laboratory C-INC, Los Alamos, NM 85745, USA.

Table 1. Decay data of the product rubidium nuclides used in this work^a.

Nuclide	Half-life	Mode of decay [%]	E_γ [keV]	I_γ [%]
$^{84\text{m}}\text{Rb}$	20.5 min	IT (100)	248.0	60.2
$^{84\text{g}}\text{Rb}$	32.8 d	EC (70) β^+ (26) β^- (4)	881.6	69.0
^{83}Rb	86.2 d	EC (100)	520.4 529.6	45.4 29.3
$^{82\text{m}}\text{Rb}$	6.3 h	EC (77) β^+ (23)	554.4 619.1	62.4 38.0
^{81}Rb	4.58 h	EC (69) β^+ (31)	190.4	64.3

a: Taken from [4].

In addition to experimental work, we performed nuclear model calculations on $^{85}\text{Rb}(p, xn)$ - and $^{85}\text{Rb}(p, pxn)$ - reactions over the energy range extending from the respective threshold up to 100 MeV. Some experimental results obtained on the isomeric cross section ratios for the isomeric pairs $^{85\text{m},\text{g}}\text{Sr}$ and $^{84\text{m},\text{g}}\text{Rb}$ are also qualitatively discussed.

2. Experimental

The techniques related to thin sample preparation, irradiations at the cyclotrons at FZ Jülich, PSI Villigen and iThemba LABS, as well as those related to beam current monitoring and measurement of the induced activity *via* high-resolution γ -ray spectrometry, have already been described [3]. Here we deal only with a few features specifically relevant to the study of the $^{85}\text{Rb}(p, pxn)$ reaction products.

Measurements on $^{84\text{m}}\text{Rb}$ ($T_{1/2} = 20.5$ min), $^{82\text{m}}\text{Rb}$ ($T_{1/2} = 6.3$ h) and ^{81}Rb ($T_{1/2} = 4.58$ h) were done using short irradiations of 30 min. For studies on $^{84\text{m}}\text{Rb}$ and $^{82\text{m}}\text{Rb}$ the samples were counted immediately after the end of irradiation since there were no disturbing genetic relationships: $^{84\text{m}}\text{Rb}$ decays 100% to the long-lived $^{84\text{g}}\text{Rb}$ and $^{82\text{m}}\text{Rb}$ decays independently to the stable ^{82}Kr , *i.e.* $^{82\text{m}}\text{Rb}$ is neither formed in the decay of ^{82}Sr nor does it decay to the ground state isomer $^{82\text{g}}\text{Rb}$ ($T_{1/2} = 1.3$ min). The results thus describe independent

formation cross sections of those two nuclides. In the case of ^{81}Rb we could not identify the 20.3 min $^{81\text{m}}\text{Rb}$ and since ^{81}Sr ($T_{1/2} = 22.2$ min) decays to $^{81\text{g}}\text{Rb}$, it was considered suitable to wait for about 4 hours before starting the counting. The results for ^{81}Rb ($T_{1/2} = 4.58$ h) thus describe cumulative cross sections, *i.e.* a sum of contributions through direct formation and parent decay.

For studies on the long-lived products ^{84}Rb ($T_{1/2} = 32.8$ d) and ^{83}Rb ($T_{1/2} = 86.2$ d) several hours' irradiations were done and the counting was started about a month thereafter to allow the short-lived products to decay. The case of ^{84}Rb was rather simple since the isomeric state decays completely to the ground state and the contribution *via* decay of the isobar ^{84}Sr is zero, the latter being stable. In the case of ^{83}Rb the measured data gave a sum of independent formation cross section and the ^{83}Sr -decay contribution. The latter could, however, be subtracted since the excitation function for the formation of ^{83}Sr ($T_{1/2} = 32.4$ h) was extensively studied in our previous work [3].

From the measured activities and the beam currents determined previously [3] the cross sections for the formation of rubidium isotopes were calculated using the well-known activation equation. The uncertainties in cross sections were also estimated as described earlier [3].

3. Nuclear model calculations

Cross sections for the formation of radioactive products were calculated using the nuclear model code ALICE-IPPE. It is a modified version of the exciton model code ALICE, originally developed by Blann [5]. The modifications introduced by the Obninsk group [6] and used here include:

- treatment of the level density in the frame of the generalised superfluid model,
- consideration of the preequilibrium cluster emission (d , t , ^3He , ^4He),
- estimation of direct interactions in cluster emission,
- calculation of γ -ray emission.

The code has been successfully applied to the calculation of (p, xn) reaction cross sections on medium and heavy mass targets [cf. 7–10]. However, more complex reactions were not reproduced well [cf. 11]. In the present work, the excitation functions of all $^{85}\text{Rb}(p, xn)$ - and $^{85}\text{Rb}(p, pxn)$ -reactions studied by us were calculated from their respective thresholds up to 100 MeV. The two cases for which calculations could not be done were the $^{85}\text{Rb}(p, n)^{85\text{m}}\text{Sr}$ and $^{85}\text{Rb}(p, pn)^{84\text{m}}\text{Rb}$ reactions since ALICE-IPPE gives only the summed cross section and not the formation of the isomeric states. In all the calculations, standard recommended input data without any additional parameter fitting were used.

4. Results and discussion

4.1 Cross section data

The measured cross section data for the reactions $^{85}\text{Rb}(p, pxn)^{84\text{m.g.}, 83, 82\text{m}, 81}\text{Rb}$ and their estimated uncertainties are given in Table 2. All values were extrapolated to 100% enrichment of the target nucleus ^{85}Rb . The results

for $^{84\text{g}}\text{Rb}$ describe cumulative cross sections, *i.e.* a sum of metastable and ground states (σ_{m} and σ_{g}). Similarly the results for ^{81}Rb also describe cumulative cross sections.

4.2 Excitation functions and comparison with the literature data

The cross sections for the reaction $^{85}\text{Rb}(p, pn)^{84\text{m}}\text{Rb}$ are shown as a function of projectile energy in Fig. 1. For comparison the data of Horiguchi *et al.* [2], measured up to 73 MeV, and those of Levkovskii [12] up to 30 MeV are also shown. The agreement between the literature data and our results is good up to about 25 MeV and in the region between 35 and 50 MeV. Between 25 and 35 MeV our values are about 30% higher than the literature data, and beyond 50 MeV our results are about 20% lower than those of Horiguchi *et al.* The results for the formation of $^{84\text{m+g}}\text{Rb}$ are given in Fig. 2. Our data are about 30% lower than the literature data.

The excitation function of the reaction $^{85}\text{Rb}(p, p2n)^{83}\text{Rb}$ is shown in Fig. 3. The data of Levkovskii [12] and

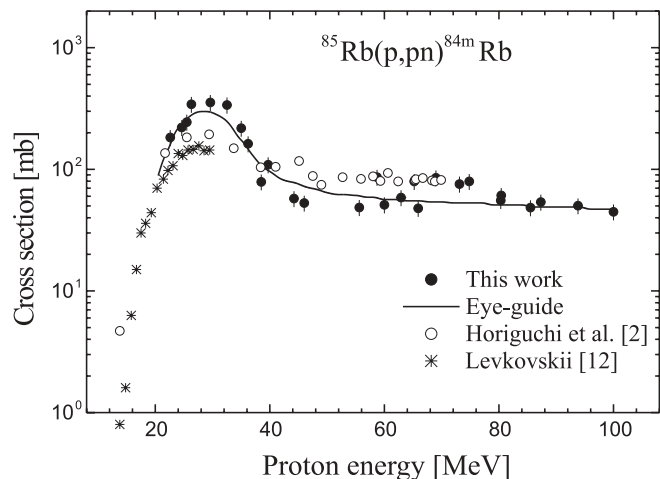


Fig. 1. Excitation function of the $^{85}\text{Rb}(p, pn)^{84\text{m}}\text{Rb}$ reaction in comparison with the data of Horiguchi *et al.* [2] and Levkovskii [12]. The curve is an eye-guide through our data points.

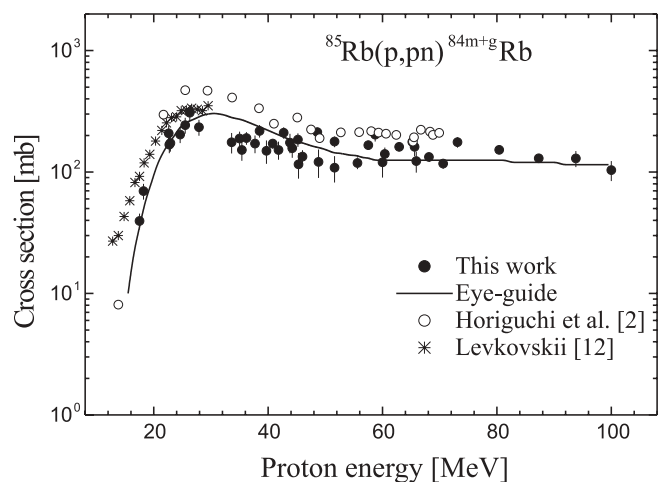


Fig. 2. Excitation function of the $^{85}\text{Rb}(p, pn)^{84\text{m+g}}\text{Rb}$ reaction in comparison with the data of Horiguchi *et al.* [2] and Levkovskii [12]. The curve is an eye-guide through our data points.

Table 2. Measured cross sections of the $^{85}\text{Rb}(p, pxn)^{84\text{m.g.}, 83, 82\text{m}, 81}\text{Rb}$ reactions.

E_p [MeV]	Reaction cross section [mb]				
	(p, pn)		$(p, p2n)$	$(p, p3n)$	$(p, p4n)$
	$^{84\text{m}}\text{Rb}$	$^{84\text{m+g}}\text{Rb}$	^{83}Rb	$^{82\text{m}}\text{Rb}$	^{81}Rb
17.5 ± 0.7		39.5 ± 5.9			
18.2 ± 0.2		69.6 ± 10.4			
22.6 ± 0.6	182.8 ± 27.4	208.4 ± 31.3			
22.7 ± 0.6		168.0 ± 25.2			
22.9 ± 0.6		173.1 ± 26.0			
24.6 ± 0.6	220.8 ± 33.1	203.7 ± 30.6	36.6 ± 5.5		
25.5 ± 0.5	244.5 ± 36.7	243.3 ± 36.5	39.2 ± 5.9		
26.3 ± 0.5	342.3 ± 51.3	307.7 ± 46.2	187.0 ± 28.1		
27.9 ± 0.5		233.8 ± 35.1	250.4 ± 37.6		
28.0 ± 0.5			153.6 ± 23.1		
29.6 ± 0.5			282.6 ± 42.4		
29.6 ± 0.5	354.9 ± 53.2		201.6 ± 30.2		
33.6 ± 0.4		176.0 ± 26.4	423.2 ± 63.5		
35.0 ± 0.4	217.9 ± 32.7	188.6 ± 28.3	541.7 ± 81.3		
35.4 ± 0.3		151.9 ± 22.8	500.5 ± 75.1	1.5 ± 0.2	
36.2 ± 0.3	162.3 ± 24.4	190.3 ± 28.6	744.9 ± 111.7		
37.7 ± 0.3		171.4 ± 25.7	611.0 ± 91.6	5.6 ± 0.9	
38.5 ± 0.3	78.9 ± 11.8	217.8 ± 32.7	714.2 ± 107.1	12.7 ± 1.9	
39.7 ± 0.3	109.1 ± 16.4	149.4 ± 22.4	473.1 ± 71.0	16.5 ± 2.5	
40.8 ± 0.2		171.5 ± 25.7	433.1 ± 65.0	32.4 ± 4.9	
41.8 ± 0.2		152.0 ± 22.8	461.2 ± 69.2	30.6 ± 4.6	0.4 ± 0.1
42.7 ± 0.2		210.7 ± 31.6	571.5 ± 85.7	60.5 ± 9.3	
43.8 ± 0.2		174.5 ± 26.2	475.5 ± 71.3	67.5 ± 10.1	1.1 ± 0.2
44.2 ± 0.2	57.5 ± 8.6	157.2 ± 23.6	407.4 ± 61.1	70.2 ± 10.5	0.5 ± 0.1
45.2 ± 0.2		184.8 ± 27.7	385.3 ± 57.8	113.9 ± 17.1	2.2 ± 0.3
45.3 ± 0.2		115.8 ± 17.4	251.5 ± 37.7	55.2 ± 8.4	1.3 ± 0.2
46.0 ± 0.5	52.8 ± 7.9	133.9 ± 20.1	341.7 ± 51.3	91.6 ± 13.7	2.5 ± 0.4
48.6 ± 0.6		212.8 ± 31.9	360.5 ± 54.1	207.5 ± 31.1	18.1 ± 2.7
51.6 ± 0.5		178.2 ± 26.7	328.7 ± 49.3	231.3 ± 34.7	34.7 ± 5.2
51.6 ± 0.5		108.6 ± 16.3	163.3 ± 24.5	147.7 ± 22.2	
55.6 ± 0.3	48.6 ± 7.3	118.7 ± 17.8	208.6 ± 31.3	119.8 ± 18.0	61.8 ± 9.3
57.5 ± 0.4		166.4 ± 25.0	243.6 ± 36.5	206.1 ± 30.9	119.6 ± 17.9
58.7 ± 1.0	86.1 ± 12.9	203.2 ± 30.5	237.1 ± 35.6	131.7 ± 19.8	142.3 ± 21.3
60.0 ± 0.2	51.1 ± 7.7	120.4 ± 18.1	189.6 ± 28.4	111.9 ± 16.8	114.7 ± 17.2
60.4 ± 0.3		140.9 ± 21.1	225.1 ± 33.8	125.3 ± 18.8	122.3 ± 18.3
62.9 ± 0.3		161.2 ± 24.2	218.7 ± 32.8	163.7 ± 24.6	174.9 ± 26.2
62.9 ± 0.9	58.6 ± 8.8			108.4 ± 16.3	146.7 ± 22.0
65.2 ± 0.8	79.6 ± 11.9	177.2 ± 26.6	173.4 ± 26.0	93.2 ± 14.0	152.2 ± 22.8
65.6 ± 0.2		161.1 ± 24.2	193.4 ± 29.0	134.5 ± 20.2	186.2 ± 27.9
65.9 ± 0.2	47.8 ± 7.2	123.0 ± 18.4	189.0 ± 28.4	93.1 ± 14.0	150.3 ± 22.5
68.1 ± 0.2		132.9 ± 19.9	198.2 ± 29.7	116.3 ± 17.4	160.1 ± 24.0
69.0 ± 0.8	85.2 ± 12.8			113.2 ± 17.0	95.7 ± 14.4
70.6 ± 0.2		117.2 ± 17.6	168.9 ± 25.3	94.1 ± 14.1	146.5 ± 22.0
73.1 ± 0.7	75.7 ± 11.4	176.4 ± 26.5	223.0 ± 33.5	106.2 ± 15.9	182.8 ± 27.4
74.8 ± 0.7	79.6 ± 11.9			127.1 ± 19.1	185.5 ± 27.8
80.3 ± 0.5	55.4 ± 8.3			106.7 ± 16.0	125.4 ± 18.8
80.4 ± 0.5	61.0 ± 9.2	152.2 ± 22.8	125.5 ± 18.8	55.9 ± 8.4	90.9 ± 13.6
85.5 ± 0.4	48.4 ± 7.3			68.4 ± 10.3	85.4 ± 12.8
87.3 ± 0.4	53.8 ± 8.1	129.8 ± 19.5	183.5 ± 27.5	57.6 ± 8.6	94.4 ± 14.2
93.8 ± 0.3	50.2 ± 7.5	129.3 ± 19.4	94.0 ± 14.1	41.0 ± 6.1	60.6 ± 9.1
100.0 ± 0.2	44.7 ± 6.7	103.7 ± 15.6	94.9 ± 14.2	45.2 ± 6.8	58.6 ± 8.8

Horiguchi *et al.* [2] are also given. There appears to be a good agreement between Levkovskii data [12] and our data. The data of Horiguchi *et al.* [2] appear to be too low by about a factor of 2 within the proton energy range of 30 to 45 MeV; beyond that energy, however, the agreement is good.

The excitation function of the $^{85}\text{Rb}(p, p3n)^{82\text{m}}\text{Rb}$ reaction is reproduced in Fig. 4. The data of Horiguchi *et al.* [2] over the energy range of 40 to 73 MeV appear to be in agreement with our values.

The excitation function of the $^{85}\text{Rb}(p, p4n)^{81}\text{Rb}$ reaction is shown in Fig. 5. The data of Horiguchi *et al.* [2] show

some energy shift and are consistently lower than our values. It is not possible to compare the present data with those of Schneider and Goldberg [1] since they concentrated on the formation of ^{81}Sr and measured the ^{81}Rb yield only *via* the decay of the parent.

4.3 Comparison of experimental and theoretical data

The experimental excitation functions of the reactions $^{85}\text{Rb}(p, xn)^{85, 83, 82, 81}\text{Sr}$ reported earlier [3] are reproduced in Fig. 6 as eye-guide curves. For comparison, the results of nuclear model calculations are also shown. The shapes of the

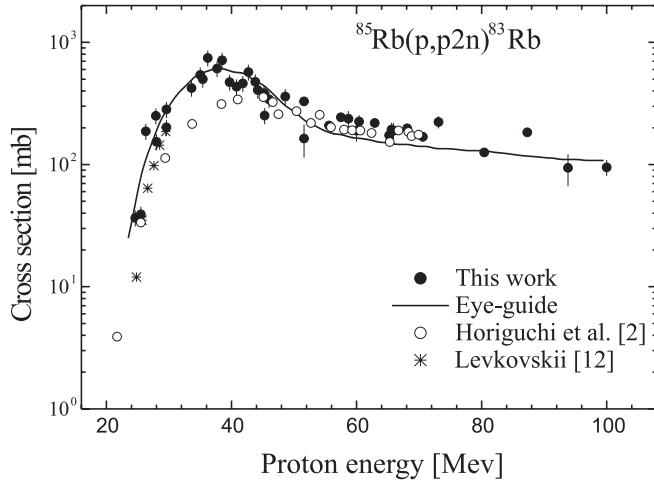


Fig. 3. Excitation function of the $^{85}\text{Rb}(p, p2n)^{83}\text{Rb}$ reaction in comparison with the data of Horiguchi *et al.* [2] and Levkovskii [12]. The curve is an eye-guide through our data points.

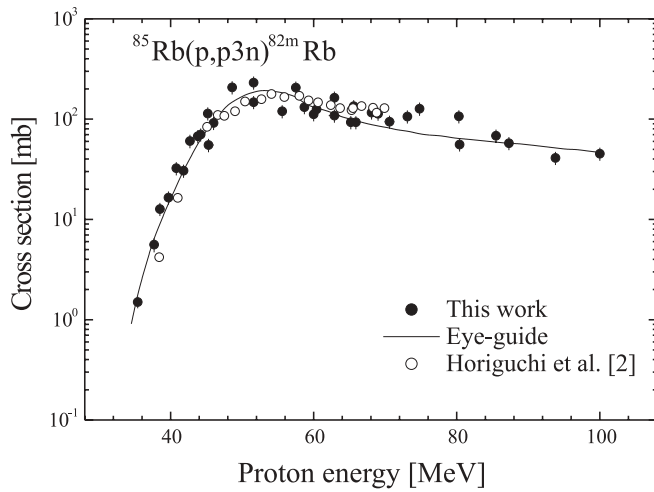


Fig. 4. Excitation function of the $^{85}\text{Rb}(p, p3n)^{82m}\text{Rb}$ reaction in comparison with the data of Horiguchi *et al.* [2]. The curve is an eye-guide through our data points.

curves appear to be described well by the calculation; the absolute cross section values, however, do not agree well. Particularly in the case of the (p, n) reaction, at incident projectile energies beyond 40 MeV the calculated cross section is much higher than the experimental value. Since the (p, n) reaction is basically a low-energy process, the extremely high calculated values at $E_p > 40$ MeV are presumably due to uncertainties in estimation of a large number of competing reaction channels.

The excitation functions of the $^{85}\text{Rb}(p, pxn)^{84,83,82m,81}\text{Rb}$ reactions measured in this work are reproduced in Fig. 7 as eye-guide curves and the results of nuclear model calculations are also given. Again the shapes of the experimental and theoretical curves agree well. The magnitudes of cross sections also agree well in the case of the $(p, p3n)$ and $(p, p4n)$ reactions leading to the formation of ^{82}Rb and ^{81}Rb , respectively. In the case of the $(p, p3n)$ reaction, this agreement is somewhat surprising since the measurement relates only to the metastable state ^{82m}Rb ($T_{1/2} = 6.3$ h) whereas the calculation gives the total cross section. Presumably the formation cross section of the ground state

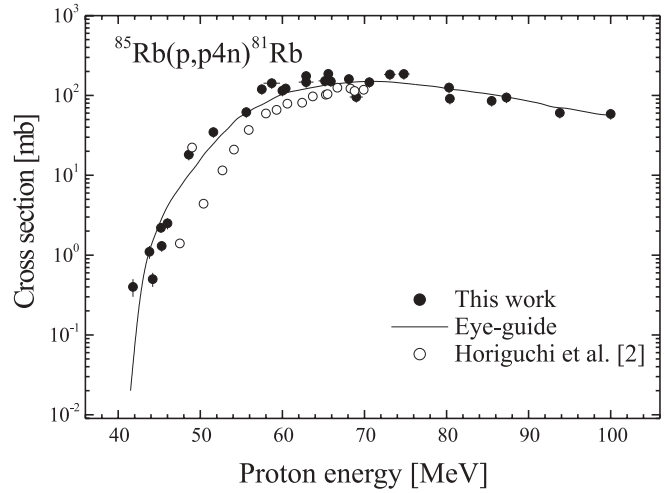


Fig. 5. Excitation function of the $^{85}\text{Rb}(p, p4n)^{81}\text{Rb}$ reaction in comparison with the data of Horiguchi *et al.* [2]. The curve is an eye-guide through our data points.

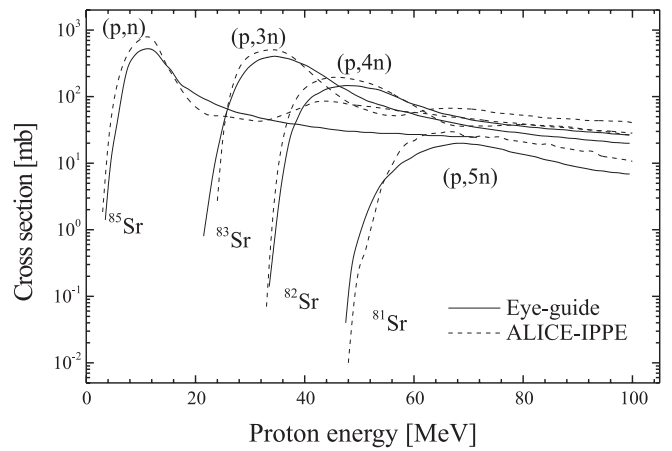


Fig. 6. Comparison of the calculated excitation functions (ALICE-IPPE) with the measured excitation functions of the $^{85}\text{Rb}(p, xn)$ -reactions given in our previous work [3].

^{82g}Rb ($T_{1/2} = 1.2$ min) is very small, so that the ^{82m}Rb formation cross section almost equals the total cross section. The experimental and theoretical excitation functions for the $^{85}\text{Rb}(p, pn)^{84}\text{Rb}$ reaction are in good agreement in the early rising part. Around the maximum and in the tail region, however, the calculated cross section values are consistently lower than the experimental data. There is considerable discrepancy in the experimental and theoretical cross sections for the formation of ^{83}Rb . The case deserves some special attention. The experimental excitation function describes a sum of $(p, p2n)$ reaction channel and the contribution *via* the decay of ^{83}Sr . The calculation, on the other hand, relates only to the $(p, p2n)$ reaction channel. Thus the discrepancy is not surprising.

From the foregoing discussion it is inferred that the experimental excitation curves and the results of nuclear model calculations on the (p, xn) and (p, pxn) reactions on ^{85}Rb are qualitatively in agreement. The (p, n) reaction in the energy region above 40 MeV is an exception. In general, however, the theory appears to reproduce the experimental excitation functions within deviations of about 50%.

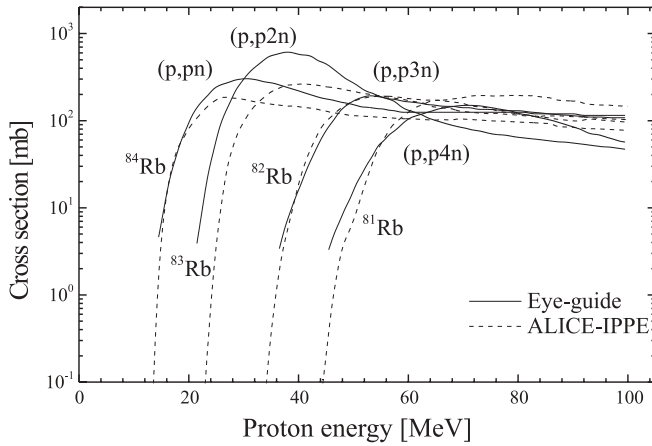


Fig. 7. Comparison of the calculated excitation functions (ALICE-IPPE) with the excitation functions of the $^{85}\text{Rb}(p, pxn)$ -reactions measured in this work. The experimental data for the formation of ^{83}Rb give a sum of the $^{85}\text{Rb}(p, p2n)$ reaction and the $^{85}\text{Rb}(p, 3n)^{83}\text{Rb} \rightarrow ^{83}\text{Rb}$ process. The calculation, however, describes only the $^{85}\text{Rb}(p, p2n)$ reaction.

4.4 Isomeric cross section ratios

In the case of two reaction channels, namely $^{85}\text{Rb}(p, n)^{85\text{m.g}}\text{Sr}$ and $^{85}\text{Rb}(p, pn)^{84\text{m.g}}\text{Rb}$, we measured the excitation functions of both the isomeric and ground states (Ref. [3] and this work). From the smooth curves, for each energy the isomeric cross section ratio $[\sigma_m/(\sigma_m + \sigma_g)]$ was deduced. The results are given in Figs. 8 and 9. Unfortunately the calculational code cannot predict isomeric cross sections. We therefore discuss the results only qualitatively.

For the pair $^{85\text{m.g}}\text{Sr}$ (Fig. 8) the isomeric cross section ratio is about 0.5 near the reaction threshold, decreasing to about 0.1 at the maximum of the excitation function, and then remaining constant over the whole investigated energy range up to 70 MeV. This means that the probability of formation of the low-spin metastable state ($1/2^-$) at low incident proton energies is about half of the total reaction channel. At higher energies this probability decreases and the higher spin isomer ($9/2^+$) is favoured.

In the case of the isomeric pair $^{84\text{m.g}}\text{Rb}$ (Fig. 9) the ratio is about 1 up to the maximum of the two exci-

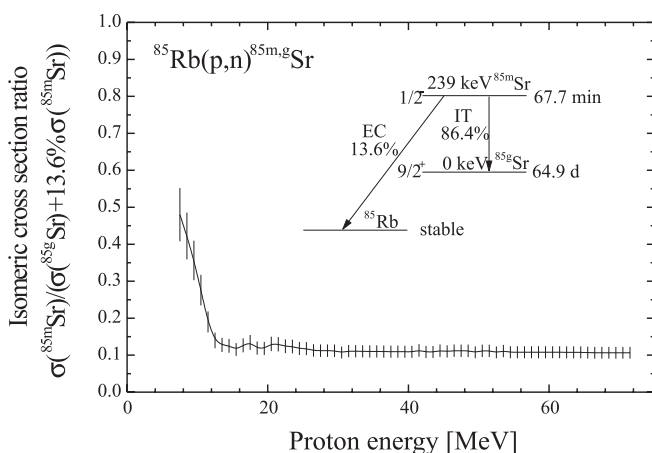


Fig. 8. Isomeric cross section ratio $[\sigma_m/(\sigma_m + \sigma_g)]$ for the isomeric pair $^{85\text{m.g}}\text{Sr}$ as a function of proton energy. The ratios were calculated from the eye-guide curves given in our previous work [3].

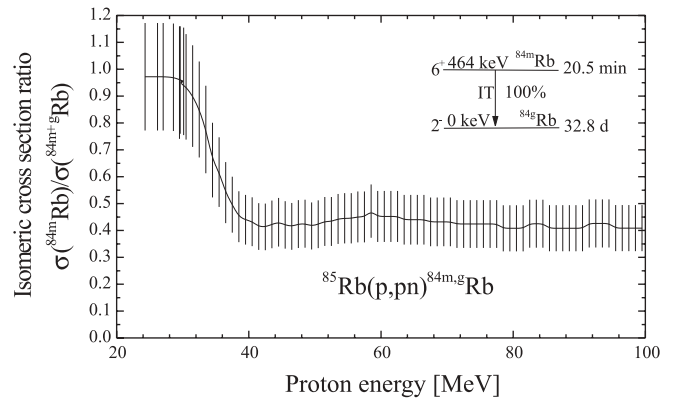


Fig. 9. Isomeric cross section ratio $[\sigma_m/(\sigma_m + \sigma_g)]$ for the isomeric pair $^{84\text{m.g}}\text{Rb}$ as a function of proton energy. The ratios were calculated from the eye-guide curves given in Figs. 1 and 2 of this work.

tation functions, decreasing to about 0.45 at higher energies, and then remaining constant till about 100 MeV. This means that the probability of formation of the high-spin isomer (6^+) is relatively high up to the maximum of the excitation function, but decreases with increasing energy. At the highest energies, where other competing reactions also occur, the probabilities of formation of the two states via the $^{85}\text{Rb}(p, pn)$ -process are more or less equal.

Acknowledgments. This work was partly carried out under a German-South African bilateral research agreement, and we thank the concerned authorities in the two countries. We also thank the operators of the four accelerators (CV 28 and Injector of COSY at the Forschungszentrum Jülich GmbH, Germany; accelerator at PSI Villigen, Switzerland; and the cyclotron at iThemba LABS, Somerset West, South Africa). Acknowledgement is made to the Deutsche Forschungsgemeinschaft (DFG), Bonn, for financial support to Yu. N. Shubin during his stay at Jülich.

References

- Schneider, R. J., Goldberg, C. J.: Production of rubidium-81 by the reaction $^{85}\text{Rb}(p, 5n)^{81}\text{Sr}$ and decay of ^{81}Sr . *Int. J. Appl. Radiat. Isot.* **27**, 189 (1976).
- Horiguchi, T., Noma H., Yoshizawa, Y., Takemi, H., Hasai, H., Kiso, Y.: Excitation functions of proton induced nuclear reactions on ^{85}Rb . *Int. J. Appl. Radiat. Isot.* **31**, 141 (1980).
- Kastleiner, S., Qaim, S. M., Nortier, F. M., Blessing, G., van der Walt, T. N., Coenen, H. H.: Excitation functions of $^{85}\text{Rb}(p, xn)^{85,83,82,81}\text{Sr}$ reactions up to 100 MeV: integral test of cross section data, comparison of production routes of ^{83}Sr and thick target yield of ^{82}Sr . *Appl. Radiat. Isot.* **56**, 685 (2002).
- Firestone, R. B.: *Table of Isotopes*. CD-ROM Edition Version 1.0, Wiley-Interscience (1996).
- Blann, M.: Preequilibrium decay. *Ann. Rev. Nucl. Sci.* **25**, 123 (1975).
- Dityuk, I., Konobeyev, A. Yu., Lunev, V. P., Shubin, Yu. N.: *New version of the advanced computer code ALICE-IPPE*. Report INDC (CCP)-410, IAEA, Vienna (1998).
- Fassbender, M., Shubin, Yu. N., Lunev, V. P., Qaim, S. M.: Experimental studies and nuclear model calculations on the formation of radioactive products in interactions of medium energy protons with copper, zinc and brass: estimation of collimator activation in proton therapy facilities. *Appl. Radiat. Isot.* **48**, 1221 (1997).
- Fassbender, M., Shubin, Yu. N., Qaim, S. M.: Formation of activation products in interactions of medium energy protons with Na, Si, P, S, Cl, Ca and Fe. *Radiochim. Acta* **84**, 59 (1999).
- Gul, K., Hermanne, A., Mustafa, M. G., Nortier, F. M., Oblozinský, P., Qaim, S. M., Scholten, B., Shubin, Yu. N., Takács, S.,

- Tárkányi, F. T., Zhuang, Y.: *Charged particle cross section database for medical radioisotope production*. IAEA – TECDOC – 1211 (2001) pp. 1–285.
10. Hohn, A., Nortier, F. M., Scholten, B., van der Walt, T. N., Coenen, H. H., Qaim, S. M.: Excitation functions of $^{125}\text{Te}(p, xn)$ -reactions from their respective thresholds up to 100 MeV with special reference to the production of ^{124}I . *Appl. Radiat. Isot.* **55**, 149 (2001).
 11. Stoll, T., Kastleiner, S., Shubin, Yu. N., Coenen, H. H., Qaim, S. M.: Excitation functions of proton induced reactions on ^{68}Zn from threshold up to 71 MeV, with specific reference to the production of ^{67}Cu . *Radiochim. Acta* **90**, 309 (2002).
 12. Levkovskii, V. N.: *Activation cross sections for the nuclides of medium mass region ($A = 40\text{--}100$) with medium energy ($E = 10\text{--}50$ MeV) protons and alpha particles (experiment and systematics)*. Inter-Vesti, Moscow, Russia (1991).